THE EFFECTIVE CONTINUUM PROPERTIES OF CARBON AND INORGANIC NANOTUBES

P. R. Heyliger, An Tran, and Fernando Ramirez
Dept. of Civil Engineering
Colorado State University, Fort Collins, CO
prh@engr.colostate.edu

Anthony Rappe' and Ian Rousom
Department of Chemistry
Colorado State University, Fort Collins, CO

Abstract

The effective mechanical continuum properties of carbon and inorganic nanotubes and their molecular sheet precursors are studied using combinations of molecular dynamics, spring-force models, finite element continuum approximations, and beam elastica. The primary features of interest are the change in properties when moving from molecular sheet to nanotube and the relative difference in these properties for different atomic structures. The three primary types of nanotube of interest in this study are carbon, boron nitride, and molybdenum sulfide.

Introduction

Nanotubes, composed of atoms typically arrayed in polygonal structure over a prismatic geometric surface, may potentially provide a means of constructing structural components that outperform their modern equivalents in strength, stiffness, and weight. There have been numerous studies within the past decade that indicate that the mechanical and electromechanical properties of these elements far exceed common structural materials, and that the gains in strength and stiffness, coupled with a drastic reduction in density, may usher in a new era of strong, lightweight components. The excitement over the novel material properties of carbon nanotubes is amplified by the recent experimental observation of organic (polyalanine), and inorganic nanotubes (boron nitride and molybdenum sulfide and numerous others). In addition to potentially having comparable strength to carbon nanotubes, inorganic and organic nanotubes possess the potential for significant electrostriction.

In this study, we model the behavior of carbon and inorganic single wall nanotubes (SWNT) over a range of three scales that represent the key physical characteristics of importance to determining the global behavior of these elements taken by themselves or as one component in a composite system. First, the nanotubes are modeled at the atomic scale using an extension of the molecular mechanics force field approach[2,25,26]. Simulations were completed for SWNT under the various types of loadings under which these elements are usually subjected: extension, compression, torsion, and flexure. The energies associated with these distortions can then be computed along with the values that yield these energies, such as bond stretching, bond angle change, torsion, and van der Waals interactions. We also use equivalent-spring models to simulate these interactions at a more reasonable computational cost. Second, an equivalent membrane-shell continuum model is used, where each layer of atoms is treated as an equivalent layer with its own material properties and thickness. This strongly localized behavior can then be used to determine the wall thicknesses and elastic constants for each layer of the representative continuum shell or fiber. The third and final representation of this class of nanotube uses the geometric and material properties of the nanotube shell model to model the nanotube as long, flexible elastica.

Since their discovery a decade ago[14], interest in carbon nanutubes has surged. Numerous theoretical predictions and physical measurements have both yielded indications that SWNT possess exceptional mechanical and electromechanical properties. A nanotube can be described as a giant linear fullerene[37], which is a closed, convex cage molecule composed strictly of hexagonal and pentagonal faces. The carbon atoms are arrayed symmetrically about the cylinder at the corners of these polygons, and the interactions between these atoms, combine to provide what may be extremely appealing strength and stiffness properties.

In the past five years the potential for nanotubular structures of other elemental combinations such as carbon boron nitrides (C_2BN), boron nitride (BN), and metal chalcoginides has been recognized and many examples synthesized. The mechanical and electrical properties of these materials are virtually unknown. Further, an examination of the literature suggests that inorganic nanotubes may have been prepared in 1961[19] and subsequently used to make 15 GPa tensile strength AlN fibers[3]. It is also likely that inorganic nanotubes are present in commercial materials such as MAO (and hence easily scaled up to bulk quantity)[10].

There have been a host of studies regarding the material behavior of both SWNT's and multi-wall nanotubes (MWNT) of carbon. Many of these studies attempt to predict the local mechanical behavior of nanotubes by matching molecular dynamics (MD) models, which take into account the interactions between adjacent carbon atoms on the cylinder, with experimental evidence from studies on relatively long nanotubes. These latter studies are usually of the form of a vibrating tube or electromechanically induced displacements. In many of these cases, the cylinder is modeled using the

assumptions of continuum mechanics, with the nanotube represented by a long, hollow cylinder of specific thickness. Other studies have increased the complexity of this class of model by representing the thickness as a single-layer, isotropic shell with a specific Young modulus and Poisson ratio. Iijima *et al.*[14] simulated the bending of both SWNT and MWNT using atomistic simulations based on Tersoff-Brenner potentials[5,34] along with a van der Waals interaction[28] between adjacent shells in MWNT or when the sides of the same shell were in close proximity. Their results, which showed excellent agreement between theory and experiment, demonstrated the formation of kinks within the tubes under increasing bending, and found that this action was fully reversible up to very large bending angles. Lu[21] computed the elastic properties of carbon nanotubes and nanoropes using the lattice-dynamical model of Al-Jishi and Dresselhaus[1], and found that the elastic moduli were insensitive to radius, number of walls, and helicity. Lu also found that the Young and shear moduli of the nanotubes were of a value similar to that of a graphite sheet, with the Young modulus of about 1 TPa computed. Although this value was nearly 5 times smaller than that reported by Yakobson et al.[39], the latter study used the π orbital extension wall thickness of 0.066 nm. Lu also used a similar methodology to study bundles of nanotubes, frequently termed ``nanoropes". These typically consist of 100-500 SWNT of uniform size and arranged in hexagonal order. Lu ignored the interactions between tubes and found very strong anisotropy, with high stiffness in the axial direction and low stiffness in the basal plane. The density of such ropes was only one half of that of graphite and one-third of that for diamond. Yao and Lordi[41] used the molecular dynamics model based on the universal force-field (UFF) developed by Rappe *et al.*[25], with bond stretching, angle bending, torsions, and inversions included in the calculations. They equated the energy as computed by the molecular model with that of a cantilever beam undergoing harmonic oscillations to compute the longitudinal Young modulus, and computed this value as around 1 TPa.

Krishnan *et al.*[17] measured the vibrations of numerous SWNT and compared the frequencies with those of Euler-Bernoulli beams with a wall thickness of 0.34 nm and diameters of 1-1.5 nm, finding a mean value for the Young modulus of 1.3 TPa. Poncharal et al.[24] matched the frequencies of electromechanically induced vibration of MWNT with those corresponding to linear Euler-Bernoulli beam theory, and found that the ``effective" bending modulus *decreased* as the wall thickness of the tube increased. They attributed this to the appearance of ripples that can appear along the inner (compressive) edge of slightly bent and relatively thick nanotubes as observed by Ruoff and Lorents[30] and others. In nearly all of these studies, a wall thickness of 0.34 nm was used based on the distance for MWNT.

In an attempt to explain some of the inconsistencies associated with using classical bending formulas with a wall thickness of 0.34 nm, Ru[29] has suggested that the effective bending stiffness of SWNT should be regarded as a material parameter independent of wall thickness, but that for MWNT the classical bending stiffness formulae may still be adequate. This argument was based primarily on the inadequacy of the Kirchhoff-Love hypothesis for thin plate/shell theory which assumes that straight-line normals remain straight and normal to a reference midplane. Ru[28] made the observation that such an assumption is limited for a shell with a thickness of a single atom. Ru[29] also demonstrated, using an elastic shell model, that van der Waals forces between layers do not increase the critical elastic strain. Another attempt to match atomic-level energies with those of a continuum was the study of Odegard *et al.*[22] for a graphene sheet. An effective thickness of around 0.28 nm was found for the case of uniaxial deformation, and 0.24 nm for pure shear.

Although most of the studies listed above have used a fixed value for the Young modulus of graphite, Krishnan *et al.*[17] have noted that the commonly accepted value of 1.02 TPa for the Young modulus of graphite is actually found from measurements on compression annealed pyrolytic graphite, and that there is wide scatter among other estimates. They further note: ``The observation of consistently higher values for Young's modulus of nanotubes as compared with bulk graphite can mean one of two things. Either the particular cylindrical structure of the graphene sheet results in increased strength, or the accepted value for graphite is underestimated. The latter is a serious possibility considering the nature of the samples used in the measurement."

Molecular Geometry

The methodology used in this study can be applied to inorganic as well as carbon nanotubes. Carbon SWNT also provide an excellent benchmark for overall material properties since they have seen such extensive study in the past few years, and they are also more readily available for experimental study than many inorganic nanotubes. Both are discussed in this work.

Carbon Nanotubes

Using the notation introduced by White *et al.*[31], a single wall of a carbon nanotube can be indexed using the integer pair (n_1,n_2) corresponding to the graphite

plane lattice vector $\mathbf{L}=n_1\mathbf{a}_1+n_2\mathbf{a}_2$. Here $\mathbf{a}_1$ and $\mathbf{a}_2$ are the unit cell vectors of the graphite sheet such as that shown in Figure 1. The nanotube is then formed by mapping this graphite sheet onto the surface of the cylinder, resulting in a radius of

$$R = \frac{a_o\sqrt{3(n_1^2 + n_2^2 + n_1 n_2)}}{2\pi}$$

where a_o=.14 nm is the length of the C-C bond. An example of the carbon nanotube is shown if Figure 2. In numerous past studies (see Lu[21], for example) the elastic constants are computed by taking the second derivatives of the strain energy density with respect to the strain components. Implicit in such calculations is the assumption of the wall thickness of the nanotube. Although it has been common to take the interlayer distance of graphite of .34 nm as the wall thickness for both SWNT and MWNT, this assumption is uncertain for carbon nanotubes and unknown for inorganic nanotubes.

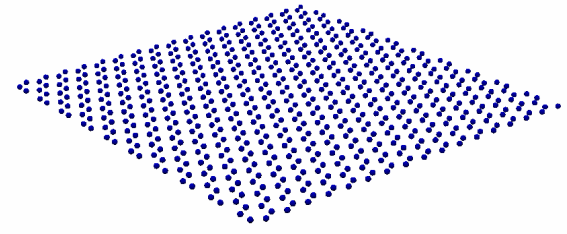

Figure 1. A molecular sheet of carbon.

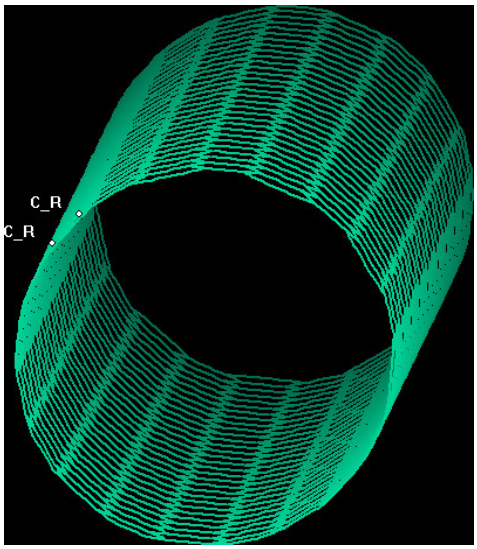

Figure 2. A representative section of a carbon nanotube.

Inorganic Nanotubes

In addition to possessing very high strength-to-weight ratios, nanotubes are observed to display fascinating electromagnetic properties. These electromagnetic properties are proposed to be important for constructing microelectronic devices as well as microelectromechanical system (MEMS) devices. Interaction of the nanotube with an applied electric field is central to both applications. For conventional insulator materials and molecules, application of an electric field will induce a dipole moment due to the polarizability:

$$\mu = \alpha_i E_i$$

For materials and molecules with a permanent dipole, the electric field can also induce a structural change (piezoelectric effect). Non-centrosymmetric (chiral) molecules and crystals intrinsically possess the potential for a dipole moment. Interestingly, modern syntheses of carbon nanotubes predominantly produce chiral nanotubes of varying helicity[14]. The third order electrical and optical response of these chiral carbon nanotubes have been the subject of theoretical and experimental studies[6,13]. The second order (polarizability) response of a chiral (zigzag and armchair) carbon nanotubes have been studied theoretically[16]. In addition to carbon nanotubes, numerous examples of nanotubular materials of other compositions have been prepared, many likely to possess interesting electrical response. Non-carbon nanotubes such as boron nitride (BN)[7] and mixed carbon boron nitrides such as C_2BN[36] have been prepared. Both small diameter[27] and large diameter[42] molybdenum sulfides have been synthesized. In principle, nanotubular materials of any layered inorganic structure, such as MoS_2, should be synthesizable leading to a wealth of materials since the crystal structures of hundreds of inorganic layered structures are known. The second order response of the non-carbon nanotubes (BN and C_2BN) have been studied theoretically, and are suggested to have polarizabilities comparable to the carbon analogs[16]. Because of the intrinsic bond polarization of non-carbon nanotubes such as boron nitride (BN) and mixed carbon boron nitrides such as C_2BN, chiral examples of these materials will possess dipole moments and should display piezoelectricity. As shown in Figure 3, inorganic nanotubes are not as stiff as carbon nanotubes (smaller Young's modulus) due to smaller bond stretch force constants and the participation of angular degrees of freedom in the deformation and hence should display a larger piezoelectric response. In this work, we quantify these properties.

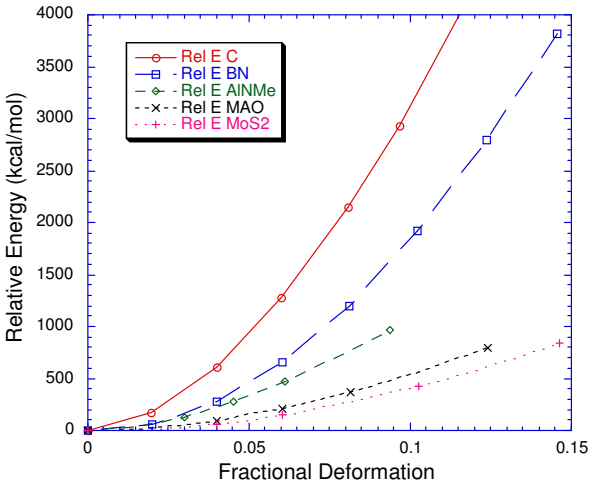

Figure 3. Energy (kcal/mol) versus fractional displacement for carbon, boron nitride, methyl aluminum methyl nitride, metlylalumoxane, and molybdenum sulfide 3 nm nanotubes. The solid line with circles corresponds to an "armchair" sample of carbon. The long dashed line with squares is for the isostructural boron nitride model, demonstating the impact that bond polarity and a decrease in bond order has on the stiffness. The medium dashed line with diamonds is of an organoaluminum nitride material first synthesized in 1961 and characterized as being polymeric at that time. Subsequent studies have documented the "cluster" nature of such materials and have used these tubular materials to synthesize high strength AlN fibers. The shorter dashed line with x's is for postulated organoaluminum oxide material that may well be present in gelled MAO. The final, shorted dashed line with +'s is for a sample derived from the electron diffraction structure of small-diameter MoS_2.

Chiral organic nanotubes have been prepared from polyalanine[40] and are likely synthesizable from helical polymers such as polyguanidine. Helical rosette nanotubes[8] have been prepared that are observed to possess tunable chiroptical properties. Due to the participation of torsional degrees of freedom in deformations of these organic materials as well as the polar nature of the carbon-nitrogen, carbon-oxygen bonding these materials should yield a significantly larger piezoelectric response than either carbon or inorganic nanotubes. MEMS devices would likely use these organic or the above inorganic nanomaterials in a polymeric matrix. Yet to be able to explore and exploit these potential opportunities, there is a need for a rapid screening tool to investigate the electrical response (polarizability and piezoelectricity) of a wide range of nanotubular materials and composites.

An example is shown in Figures 4-6 for molybdenum sulfide, with two views of the parent molecular sheet in Figures 4 and 5, and the final end view of a corresponding nanotube section in Figure 6.

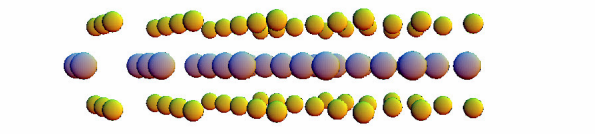

Figure 4. A molecular sheet of molybdenum sulfide (the yellow atoms represent the sulfide).

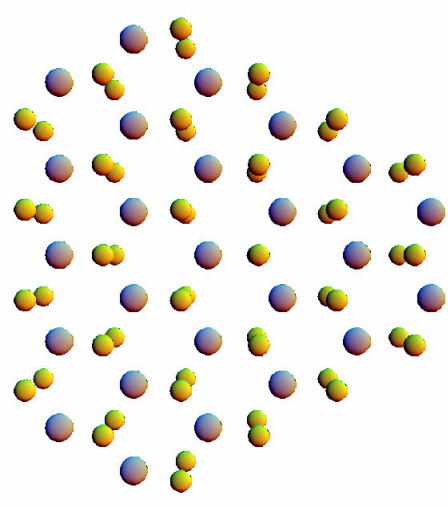

Figure 5. Top view of the molecular sheet of molybdenum sulfide.

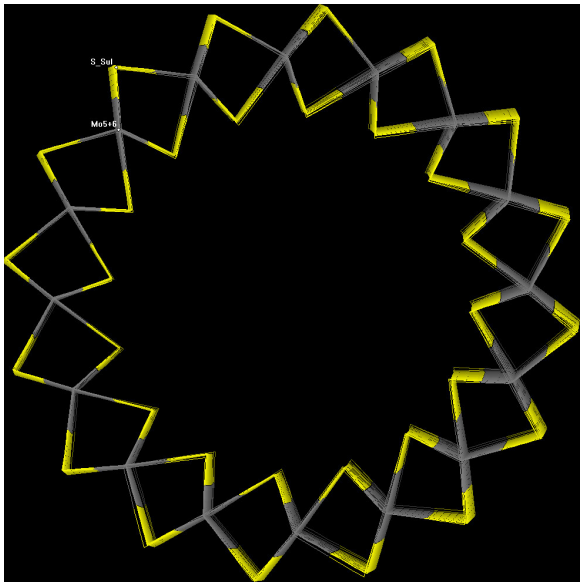

Figure 6. End view of a molybdenum sulfide nanotube section.

An additional example is shown in Figure 7, with a nanotube of aluminum-oxygen-methyl shown. The nanotubes in these figures raise interesting questions related to the effective continuum properties when

considering the mechanics of these elements. Unlike the nanotubes of carbon and BN, these molecules possess no clear point of origin for an effective shell thickness. At this point it remains to be seen what continuum representations best mimic the global response characteristics for a various range of tubes geometry.

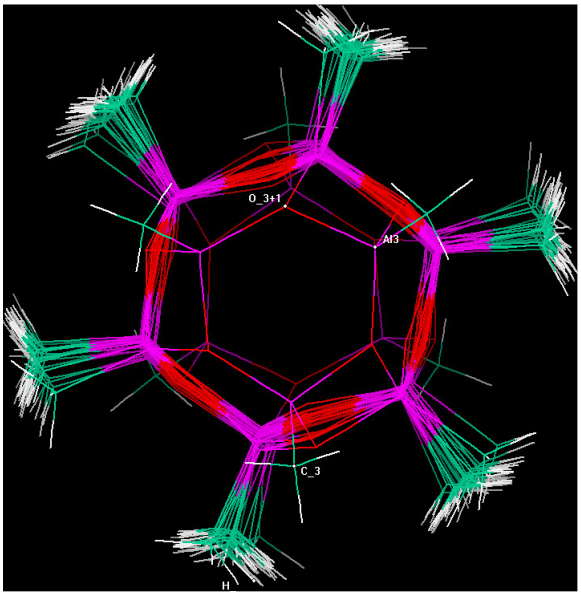

Figure 7. End view of aluminum-oxygen-methyl nanotube.

Nanotube Models

Molecular Mechanics

The potential energy for a molecule is the sum of energies from two, three, and four-body interactions (Rappe'[26]), and can be expressed as

$$E = E_R + E_\theta + E_\phi + E_\omega + E_{vdw} + E_{el}$$

The first four energies on the right-hand side of this equation are related to bond stretching, bond angle bending, dihedral angle torsion, and inversion terms, respectively. The nonbonded energies include van der Waals and electrostatic contributions as represented by the final two terms on the right-hand side. In carbon nanotubes, there is no net charge associated with the carbon atoms, and hence E_{el}=0. However, for boron nitride, molybdenum sulfide, or other organic or inorganic materials electrostatics should play a role, and in fact this should generate a bulk piezoelectric effect that can be exploited to use the inorganic nanotubes as sensors/actuators either acting alone or within a matrix to form an adaptive composite.

In conventional molecular mechanics, the bond stretch energy can be expressed as the sum of force constants multiplied by the square of the bond stretch between carbon atoms as

$$E_R = \frac{1}{2}\sum_{IJ} K^R_{IJ}(r - r_{IJ})^2$$

where K^R_{IJ} is the force constant with units of (kcal/mol)/A^2 and r_{IJ} is the natural bond length in angstroms. The current methodology uses an Extended Rydberg bond stretch and bond order-dependent angular terms to provide a proper description of large motion deformations and permit bond dissociation. A Morse-6 vander Waals potential is used and the electrostatic model includes atomic as well as bond polarization.

The parameters K^R_{IJ} and r_{IJ} in the above expression are dependent upon the elements involved in the bond and the type of bond (single, double, triple, etc.). In the interest of brevity, we do not explicitly state the form of the remaining energy terms, but merely state that they have similar forms to those for bond stretch energy. In each of these terms, the potential energy is related to the change in position of adjacent atoms for a specific deformation field.

Pin-Spring Models

The basic idea behind pin-spring models is to simulate the bond stretch, bond angle change, bond torsion, and other effects from a molecular mechanics model by an equivalent system of rods and springs[4]. By applying a forcing function to the pin-spring model, the deformation characteristics should be similar to those obtained by integrating Netwon's equations of motion at the atomic scale, but is usually completed at a fraction of the computational cost. Although there are losses in accuracy, the increase in computational speed can sometimes be of benefit where a large number of simulations are necessary.

To date, the study of nanotubes by such models have been fairly limited. Examples include the work of Odegard *et al.*[22,23], which yielded two different estimates for the thickness of graphene, and Li and Chou[20], who modeled the strength of carbon tubes using atomistic modeling. Our model differs from these approaches by representing angle changes in terms of the atomic displacements, which is analytically tedious but computationally advantageous.

The potential energy of the bond angle change can be given a structural analog using a torsional spring. For the two line elements in a plane, we define the local node

triplets along with the displacement components Δ_1-Δ_4. For small angle approximations, the total angle change can be expressed in terms of these four displacement components along with the element lengths L_1 and L_2. Hence the potential energy stored in the torsional spring can be expressed as

$$\Pi_\theta = \frac{1}{2} k_\theta \left(\frac{\Delta_2}{L_1} + \frac{\Delta_3}{L_2} - \frac{\Delta_1}{L_1} - \frac{\Delta_4}{L_2} \right)^2 \quad (4)$$

where the displacement components can be expressed in terms of the end-node displacements as

$$\Delta_1 = u_1 n_x + v_1 n_y + w_1 n_z$$
$$\Delta_2 = u_2 n_x + v_2 n_y + w_2 n_z$$
$$\Delta_3 = u_1 \bar{n}_x + v_1 \bar{n}_y + w_1 \bar{n}_z$$
$$\Delta_4 = u_3 \bar{n}_x + v_3 \bar{n}_y + w_3 \bar{n}_z$$

Here n_i and $\bar{n}_i$ are the components of the two unit vectors normal to each of the line elements. If we define the vectors $\mathbf{t}_1$ and $\mathbf{t}_2$ as the unit tangent vectors of each of the line elements and the vector $\mathbf{n}_3$ as the unit vector normal to the plane containing the two line elements, the components of the unit normal vectors $\mathbf{n}$ and $\bar{n}$ can be expressed as

$$\hat{\mathbf{n}} = (n_{32}t_{13} - n_{33}t_{12})\hat{\mathbf{e}}_1 + (n_{33}t_{11} - n_{31}t_{13})\hat{\mathbf{e}}_2 + (n_{31}t_{12} - n_{32}t_{11})\hat{\mathbf{e}}_3$$

and

$$\hat{\bar{\mathbf{n}}} = (n_{32}t_{23} - n_{33}t_{22})\hat{\mathbf{e}}_1 + (n_{33}t_{21} - n_{31}t_{23})\hat{\mathbf{e}}_2 + (n_{31}t_{22} - n_{32}t_{21})\hat{\mathbf{e}}_3$$

where t_{1i} is the i-th component of the vector $\mathbf{t}_1$. Manipulation of these terms results in a rotational stiffness matrix added to the bond-element matrix typically generated for this sort of analysis[22].

Continuum Shell Membrane Model

The microstructure of many nanotubes is consistent with that of a rolled hexagonal lattice. This is a geometry that can be modeled as a shell or collection of planar membrane elements, with both approaches used by various researchers. We use a continuum based membrane shell model that will allow us to determine the effective geometry and material properties of these nanotubes more carefully. We represent the molecular sheet and nanotubes as collections of finite piezoelectric membrane elements, for which the difference in field (local) and energy (global) values are minimized to determine the optimal effective properties.

The Elastica

Most studies of global nanotube mechanics have invoked the assumptions consistent with infinitesimal deformations and strains once the molecular model has been replaced with a continuum beam description. To our knowledge, no studies have been completed in which the large deflections of the nanotubes are taken into account as part of the study of the mechanics of these elements (such as modeling the already observed nanotube tied in a knot). Such a representation may be critical. Poncharal *et al.*[24] measured static deflections of carbon nanotubes induced by an electric field, and found that SWNT with D=20 nm could be bent to a radius of smaller than 80 nm without exceeding the elastic limit. Although several studies have examined, for example, local buckling behavior of nanotubes, many applications (such as sensors) require nanotubes with lengths hundreds or thousands of times greater than the nanotube diameter. The ability to model these elements as they deform into a shape exceeding that of linear Euler-Bernoulli beam theory is a critical thrust which has not seen any study to date. We model the nanotube as an elastica elements with the capability to withstand large deformations but only small strains since the diameter/length ratio is so small and even large deformations will generate small strains. We formulate the problem for elastica elements given the cross-sectional properties determined in our previous steps.

Results

For several of the nanotube configurations, the molecular sheet provides an initial configuration worthy of study as many of the same principles apply to these structures as do the final nanotubes. The molecular sheet also provides a means of comparison when computing the effective continuum properties of these elements.

Carbon

The carbon sheet has been studied by several researchers using several different models. Kudin, Scuseria, and Yakobson[18] found a value for $C=Yh=345 J/m^2$, where Y is the Young modulus and h the sheet thickness of graphene, along with a Poisson ratio of 0.149 using *ab initio* models. Odegard *et al.*[22] used pin-spring models to study the graphene sheet, and combined the bulk properties of graphite of Y = 1030 GPa and ν= 0.17, examined planar motion of a representative volume element to find a sheet thickness of 0.28 nm under axial extension and 0.24 nm under

shear deformation. As noted by Odegard *et al.*, numerous other researchers have used a value of 0.34 nm for carbon nanotube thickness.

As a simple first example, we re-examine the graphene sheet composed of carbon atoms on a sheet, as studied by Odegard et al[24]. Using the distance between atoms of 0.14 nm and the axial force and bond angle constants of 46900 kcal/mole-nm^2 and 63 kcal/mole-rad^2, respectively, we impose affine motion on a molecular carbon sheet and determine the energy stored using the pin-spring model we have developed and a continuum representation of the energy. In the latter case, the energy is calculated by dividing the hexagon into two common plane-stress elements and computed the strain energy using the bulk properties of graphite. The displacements are computed using constant strain in the x and y directions, and then repeated using pure shear deformation under the conditions of affine motion, expressed as

$$u_i = \varepsilon_{ij} x_j$$

The sheet thicknesses we compute using this approach are very consistent, giving values of 0.3024 nm for both cases of extensional strain and 0.3018 nm for the case of pure shear. These values contrast with the values of Odegard *et al.* of 0.28 nm and 0.24 nm for the extensional and shear cases, respectively. (We replicated these values, finding 0.277 nm and 0.2359 nm for the extensional and shear cases using the model of Odegard *et al.*). We also consider the case of pure dilatation, finding an effective thickness of 0.3033 nm for our model versus a value of 0.334 nm for that of Odegard *et al.* The primary reason for this difference is that our model contains energy only by bond stretching for pure dilatation, whereas the model of Odegard *et al.* contains energy from both bond stretch and equivalent angle changes, resulting in more thickness required to match the energy.

We then extend this procedure to a carbon nanotube. Using a molecular force model, a tube with 680 atoms was subjected to axial strain and the change in energy then computed. Using the atomic displacements, we then represented the nanotube using 4-noded plane elasticity elements (under plane stress conditions) and imposed the exact value of the nodal displacements on this continuum. We then assume that the in-plane properties of the molecular sheet are close to those of the nanotube. This assumption has not yet been subjected to convincing study, but indications from first-principles studies of the radial breathing modes of SWNT indicate that the elastic constants change very little when the sheet is rolled into a nanotube. The computed thickness for the wall was 0.233 nm, indicating that the change in geometry from sheet to tube results in decrease in effective thickness or an increase in stiffness.

It is also possible to examine the mechanics of deformation of the molecular sheet without using the bulk properties of graphite. We do this with carbon to develop estimates for the graphene Poisson ratio and effective in-plane stiffness (or Young modulus multiplied by thickness). The lattice used is that shown in Figure 1. Our approach is complicated when using the molecular force model by not being able to constrain the displacements of the atoms along the edges to conform with a uniform transverse strain given a fixed longitudinal strain since the Poisson ratio is unknown. To circumvent this difficulty, we apply a known strain in the x-direction and then allow relaxation of the atoms in the y-direction a fixed amount. We repeat this procedure using several different values of transverse displacement, and then select the configuration corresponding to a minimum of potential energy. Using this approach, we obtain values of Poisson ratio of 0.21 and 0.22 in the two directions of the lattice, given a slightly larger value than those reported using ab initio methods.

The Nanotube as Elastica

It is common to use the effective stiffness (Young modulus multiplied by thickness) when studying nanotubes because of the uncertain nature of the tube wall thickness. However, there are some applications where an idea of effective wall thickness is important in nanotube mechanics. One of these situations exists when the nanotube is treated as a bar/beam element undergoing large deformations (but usually small strains). Such a problem was first considered by Euler, who applied the label of ``elastica'' to this class of problem. In cases such as this, the differential equations that link the axial and bending behavior of the element that uncouple under small displacements are now coupled as the beam displacement becomes large. Under these conditions, the strain energy from flexure is no longer a function of the linearized curvature, but now takes the more complicated form

$$\pi = \int_V \frac{EIw''}{\left[1 + w'^2 R\right]^{5/2}} dx$$

There are a number of methods that can be used to compute the deflected shape. We omit details of our approach here, but state generally that they follow the methodology of Yang.

We use the properties of the tube described in the previous section (E=1030 Gpa, r=0.674 nm, t=0.2327 nm) and consider the problem of a tip-loaded cantilever

beam and a fixed-fixed beam loaded mid-span modeling the nanotube as an elastica. The results of the displacements, and the variance with linear theory, are shown in Figures 8 and 9.

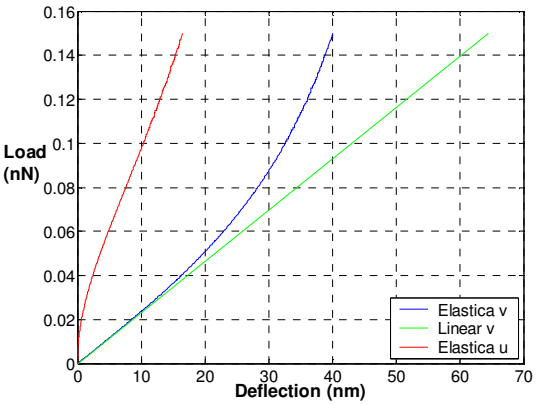

Figure 6. The load-deflection response of a tip-loaded cantilever carbon nanotube modeled as an elastica with length to diameter ratio L/d=100. In the figure u represents the horizontal displacement of the cantilever tip, while v represents the vertical displacement of the cantilever tip.

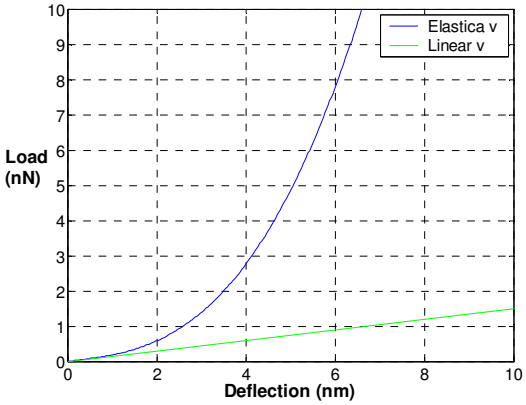

Figure 7. The load-deflection response for a fixed-fixed carbon nanotube modeled as an elastica beam subjected to a concentrated load at the mid-span, with length to diameter ratio L/d=100. In the figure v represents the vertical displacement at the mid-span of the beam.

Conclusions

Using a combination of molecular, pin-spring, continuum, and elastica models, our preliminary results indicate that:

1. There is an increase in effective stiffness when moving from sheet to tube for carbon.
2. The bulk Poisson ratio of a carbon sheet is approximately 0.21.
3. The modeling of nanotubes as conventional beams should be approached with caution, as under certain loading conditions the behavior ceases to be geometrically linear at fairly small effective loads.

Appendix

The first row of the element matrix for the bond-angle change terms in the pin-spring analysis can be expressed in terms of the element bond lengths and their unit normal vector components. These are expressed as

$$k_{11}^{\theta} = \frac{n_x^2}{L_1^2} + \frac{\bar{n}_x^2}{L_2^2} - \frac{2n_x\bar{n}_x}{L_1L_2}$$

$$k_{12}^{\theta} = \frac{n_x n_y}{L_1^2} - \frac{n_y\bar{n}_x}{L_1L_2} - \frac{n_x\bar{n}_y}{L_1L_2} + \frac{\bar{n}_x\bar{n}_y}{L_2^2}$$

$$k_{13}^{\theta} = \frac{n_x n_z}{L_1^2} - \frac{n_z\bar{n}_x}{L_1L_2} - \frac{n_x\bar{n}_z}{L_1L_2} + \frac{\bar{n}_x\bar{n}_z}{L_2^2}$$

$$k_{14}^{\theta} = \frac{n_x\bar{n}_x}{L_1L_2} - \frac{n_x^2}{L_1^2}$$

$$k_{15}^{\theta} = \frac{n_y\bar{n}_x}{L_1L_2} - \frac{n_x n_y}{L_1^2}$$

$$k_{16}^{\theta} = \frac{n_z\bar{n}_x}{L_1L_2} - \frac{n_x n_z}{L_1^2}$$

$$k_{17}^{\theta} = \frac{n_x\bar{n}_x}{L_1L_2} - \frac{\bar{n}_x^2}{L_2^2}$$

$$k_{18}^{\theta} = \frac{n_x\bar{n}_y}{L_1L_2} - \frac{\bar{n}_x\bar{n}_y}{L_2^2}$$

$$k_{19}^{\theta} = \frac{n_x\bar{n}_z}{L_1L_2} - \frac{\bar{n}_x\bar{n}_z}{L_2^2}$$

References

[1] Al-Jishi, R., and Dresselhaus, G. (1982), "Lattice-dynamical model for graphite," *Phys. Rev. B* **26**, pp. 4514-4522.

[2] Allinger, N. L., Yuh, Y. H., and Lii, J. H. (1989), "Molecular Mechanics. The MM3 force field for hydrocarbons," *J. Am. Chem. Soc.* **111**, pp. 8551-8566.

[3] Bolt, J. D.,Tebbe, F. N. (1996), US Patent 5,508,239.

[4] Born, M., and Huang, K., *Dynamical Theory of Crystal Lattices*, Oxford University Press, London (1954).

[5] Brenner, D. W. (1990), "Empirical potential for hydrocarbons for use in simulating the chemical vapor deposition of diamond films," *Phys. Rev. B* **42**, pp. 9458-9471.

[6] Chen, Y.-C., Raravikar, N. R., Schadler, L. S., Ajayan, P. M., Zhao, Y.-P., Lu, T.-M., Wang, G.-C., Zhang, X.-C. (2002), "Ultrafast optical switching properties of single-wall carbon nanotube polymer composites," *Applied Physics Letters* **81**, pp. 975-977.

[7] Chopra, N. G., Luyken, R. J., Cherrey, K., Crespi, V. H., Cohen, M. L., Louie, S. G., Zettl, A. (1995), "Boron nitride nanotubes," *Science* **269**, pp. 966-967.

[8] Fenniri, H., Deng, B.-L., Ribbe, A. E. (2002), "Helical Rosette Nanotubes with Tunable Chiroptical Properties," *J. Am. Chem. Soc.* **124**, pp. 11064-11072.

[9] Goldberg, D., Bando, Y., Bourgeois, L., Kurashima, K., and Sato, T. (2000), "Insights into the structure of BN nanotubes," *Applied Physics Letters* **77**, pp. 1979-1981.

[10] Harlan, C. J., Bott, S. G., Barron, A. R. (1995), "Three-Coordinate Aluminum is Not a Prerequisite for Catalytic Activity in the Zirconocene-Alumoxane Polymerization of Ethylene," *J. Am. Chem. Soc.* **117**, pp. 6465-6474.

[11] Hernandez, E., Goze, C., Bernier, P.,and Rubio, A. (1998), "Elastic properties of C and $B_xC_yN_z$ composite nanotubes," *Phys. Rev. Lett.* **80**, pp. 4502-4505.

[12] Jensen, L., Schmidt, O. H., Mikkelsen, K. V. (2002) "Static and Frequency-Dependent Polarizability Tensors for Carbon Nanotubes," *J. Phys. Chem. B* **104**, pp. 10462-10466.

[13] Jiang, J., Dong, J., Xing, D. Y. (1999), "Size and helical symmetry effects on the nonlinear optical properties of chiral carbon nanotubes," *Phys. Rev. B* **59**, pp. 9838-9841.

[14] Iijima, S. (1991), "Helical microtubules of graphitic carbon," *Nature* **354**, pp. 56-58.

[15] Iijima, S., Brabec, C., Maiti, A., and Bernholc, J. (1996), "Structural flexibility of carbon nanotubes," *J. Chem. Phys.* **104**, pp. 2089-2092.

[16] Kongsted, J., Osted, A., Jensen, L., Astrand, P.-O., Mikkelsen, K. V. (2001) *J. Phys. Chem.* **105**, pp. 102443-10248.

[17] Krishnan, A., Dujardin, E., Ebbesen, T. W., Yianilos, P. N., and Treacy, M. M. J. (1998), "Young's modulus of single-walled nanutubes," *Phys. Rev. B* **58**, pp. 14013-14019.

[18] Kudin, K. N., Scuseria, G. E., and Yakobson, B. I. (2001), "C_2F, BN, and C Nanoshell Elasticity from *ab initio* Computations," Phys. Rev. B. **64**, p. 235406.

[19] Laubengayer, A. W., Smith, J. D, Ehrlich, G. G. (1961), "Aluminum-Nitrogen Polymers by Condensation Reactions," *J. Am. Chem. Soc.* **83**, pp. 542-546.

[20] Li, C., and Chou, T.-W., "An Atomistic-Modeling of Carbon Nanotube Tensile Strength," Paper AIAA-2002-1520, Proceedings of the 59th SDM Conference, Denver, CO (2002).

[21] Lu, J. P. (1997), "Elastic properties of carbon nanotubes and nanoropes," *Physical Review B* **79**, pp. 1297-1300.

[22] Odegard, G. M., Gates, T. S., Nicholson, L. M., and Wise, K. E. (2001), "Equivalent-continuum modeling of nano-structured materials," NASA/TM-20010219863.

[23] Odegard, G. M., Gates, T. S., Wise, K. E., Park, C., and Siochi, E. J. (2001), "Constitutive Modeling of Nanotube-reinforced Polymer Composites," NASA/CR-20020211760.

[24] Poncharal, P., Wang, Z. L., Ugarte, D., and de Heer, W. A. (1999), "Electrostatic deflections and electromechanical resonances of carbon nanotubes," *Science* **283**, pp. 1513-1516.

[25] Rappe', A. K., Casewitt, C. J., Colwell, K. S., Goddard III, W. A., and Skiff, W. M. (1992), "UFF, a Full Periodic Table Force Field for Molecular Mechanics and Molecular Dynamics Simulations," *J. Am. Chem. Soc.* **114**, pp. 10024-10035.

[26] Rappe', A. K., and Casewit, C. J. (1997), "Molecular Mechanics across Chemistry," *University Science Books*, Sausalito, California.

[27] Remskar, M., Mrzel, A., Skraba, Z., Jesih, A., Ceh, M., Demsar, J., Stadelmann, P., Levy, F., Mihailovic, D. (2001), "Self-Assembly of Subnanometer-Diameter Single-Wall MoS2 Nanotubes," *Science* **292**, pp. 479-481.-

[28] Ru, C. Q. (2000), "Effect of van der Waals forces on axial buckling of a double-walled carbon nanotube," *J. Appl. Phys.* **87**, pp. 7227-7231.

[29] Ru, C. Q. (2000), "Effective bending stiffness of carbon nanotubes," *Phy. Rev. B* **62**, pp. 9973-9976.
[30] Ruoff, R. S., and Lorents, D. C. (1995), *Carbon* **33**, pp. 925-930.
[31] Saito, R., Dresselhaus, G., and Dresselhaus, M. S. (1988), *Physical Properties of Carbon Nanotubes*, Imperial College Press, London.
[32] Tada, Y., and Lee, G. C. (1970), "Finite element solution to an elastica problem of beams," *Int. J. Num. Meth. Eng.* **2**, pp. 229-241.
[33] Tenne, R., and Zettl, A. K. (2001), ``Nanotubes from inorganic materials," *Top. Appl. Phys.* **80**, pp. 81-112.
[34] Tersoff, J. (1986), "New empirical model for the structural properties of silicon," *Phys. Rev. Lett.* **56**, pp. 632-635.
[35] Van Lier, G., Van Alsenoy, C., Van Doren, V., and Geerlings, P. (2000), "Ab initio study of the elastic properties of single-walled carbon nanotubes and graphene," *Chem. Phys. Lett.* **326**, pp. 181-185.
[36] Weng-Sieh, Z.; Cherrey, K.; Chopra, Nasreen G.; Blase, X.; Miyamoto, Yoshiyuki; Rubio, Angel; Cohen, Marvin L.; Louie, Steven G.; Zettl, A.; Gronsky, R. (1995), "Synthesis of BxCyNz nanotubules," *Phys. Rev. B* **51**, pp. 11229-32.
[37] Wong, E. W., Sheehan, P. E., and Lieber, C. M. (1997), "Nanobeam mechanics: elasticity, strength, and toughness of nanorods and nanotubes," *Science* **277**, pp. 1971-1974.
[38] Yakobson, B. I., and Smalley, R. E. (1997), "Fullerene nanotubes: $C_{1,000,000}$ and beyond," *American Scientist* **85**, pp. 324-337.
[39] Yakobson, B. I., Brabec, C. J., and Bernholc, J. (1996), "Nanomechanics of carbon tubes: instabilities beyond the linear range," *Phys. Rev. Lett.* **76**, pp. 2511-2514.
[40] Yang, T. Y. (1973), "Matrix displacement solution to elastic problems of beams and frames,'' *Int. J. Solids. Struct.,* **9**, pp. 829-942.
[41] Yang, Y., Wan, M. (2002), "Chiral nanotubes of polyaniline snthesized by a template-free method," *J. Mater. Chem.* **12**, 897-901.
[42] Yao, N., and Lordi, V. (1998), "Young's modulus of single-walled carbon nanotubes," *J. Appl. Phys.* **84**, pp. 1939-1943.
[43] Zelenski, C. M. Dorhout, P. K. (1998), "Template Synthesis of Near-Monodisperse Microscale Nanofibers and Nanotubules of MoS2," *J. Am. Chem. Soc.* **120**, pp. 734-742.